Formation of plutonium(iv) silicate species in very alkaline reactive media

Paul Estevenon, Thomas Dumas, Pier Lorenzo Solari, Eleonore Welcomme, Stephanie Szenknect, Adel Mesbah, Kristina Kvashnina, Philippe Moisy, Christophe Poinssot, Nicolas Dacheux

ARTICLE

Formation of plutonium (IV) silicate species in very alkaline reactive media

Received 00th January 20xx,
Accepted 00th January 20xx

DOI: 10.1039/x0xx00000x

Paul Estevenon[a,b,c,d], Thomas Dumas[a,*], Pier Lorenzo Solari[e], Eleonore Welcomme[a], Stephanie Szenknect[b], Adel Mesbah[b], Kristina O. Kvashnina[c,d], Philippe Moisy[a], Christophe Poinssot[a], Nicolas Dacheux[b,*]

Studying the speciation of Pu(IV) in very alkaline and silicate ions rich reactive media allowed identifying the formation of plutonium (IV)-silicate colloidal suspensions which were stable for months. These colloids were stabilized in aqueous solution for pH > 13 and for concentrations around 10^{-2} mol·L^{-1}. Successive filtration process allowed evaluating their size, which was found to be smaller than 6 nm. Their structural characterization by XAS evidenced that their structure was similar to those identified for the other tetravalent actinide-silicate colloidal systems like thorium, uranium and neptunium. Their formation could explain the increase of plutonium solubility usually observed in alkaline silicate-rich solutions and could affect the plutonium mobility as instance in contaminated sites or in other environmental permeable media.

Introduction

Actinides, and mainly plutonium, are the main contributors to the long-term radiotoxicity of spent nuclear fuel.[1] In conditions representative of a geological repository, the interactions between such radioelements and silicate species could influence the mobility of the actinides in the environment [2-4] and thus, could affect the safety of the nuclear waste repository facilities.

Even if the formation of plutonium silicate complexes and solid plutonium silicate species (or that of other actinide or surrogate elements) has been reported,[5-12] plutonium (IV) chemistry in silicate environment remains poorly understood. Among them, $Pu(OSi(OH)_3)^{3+}$ was prepared between pH 0.3 and 1.4 in diluted aqueous plutonium and silicate solution and a log(β°) = 11.8 (1) value was evaluated according to equation (1).[5]

$$Pu^{4+} + H_3SiO_4^- \leftrightharpoons Pu(OSi(OH)_3)^{3+} \quad \textbf{(1)}$$

Pazukhin *et al.*[6] observed that the titration of Pu(IV) in nitric solution by a aqueous sodium metasilicate solution did not lead to the precipitation of plutonium hydroxide up to pH = 12 while its precipitation occurred at pH = 2 – 4 for a titration performed with NaOH or NH_4OH without metasilicate. They attributed these results to the formation of a plutonium silicate complex with a $[Pu(IV)]:[Na_2SiO_3] = 1:8$ mole ratio.[6] However, these results and especially the pH values reported should be considered with caution. Indeed, the Pu(IV) hydrolysis and the precipitation of plutonium hydroxide generally occurs below pH = 1 in non-complexing reactive media.[13] Moreover, the UV-visible spectra obtained are very similar to those reported by Yusov *et al.* for $Pu(OSi(OH)_3)^{3+}$.[5] Shilov and Fedoseev [14] also observed that silicate species have an impact on the Pu(IV) solubility in alkaline conditions, pH = 11 – 13.8, leading to plutonium concentrations around 10^{-8} mol·L^{-1},[14] after ultrafiltration with 10 kDa filters (i.e. pores diameter 2.8 nm),[15] against 4×10^{-11} mol·L^{-1} in silicate free reactive media.[13] This increase of solubility was attributed to the potential formation of $Pu^{IV}(SiO_3)_n^{(4-2n)}$ species following reaction (2). However, Shilov and Fedoseev didn't observe any impact of silicate ions on plutonium solubility at pH = 9, unlike the results reported by Pazukhin *et al.*.[6]

$$Pu^{4+} + nSiO_3^{2-} \leftrightharpoons Pu(SiO_3)_n^{(4-2n)} \quad \textbf{(2)}$$

Experiments performed with thorium(IV) and neptunium(IV) in silicate reactive media also led to the formation of $An(OSi(OH)_3)^{3+}$ complexes.[5, 16] Moreover, silicate ions have been identified to have a strong impact on thorium solubility in alkaline reactive media due to the formation of a thorium hydroxo-silicate complex, $[Th(OH)_3(OSi(OH)_3)_3]^{2-}$, which has been evidenced in these conditions.[17]

Furthermore, the formation of actinide silicate colloids has been reported for thorium(IV),[2, 18-21] uranium(IV) [3, 20-23] and neptunium(IV) [4, 21, 24] (**Table 1**). The stability and mobility of these actinide bearing silicate colloids under environmental conditions strongly differed from the oxy-hydroxide colloids

[a] CEA, DES, ISEC, DMRC, Univ Montpellier, Marcoule, France.
[b] ICSM, Univ Montpellier, CNRS, CEA, ENSCM, Bagnols-sur-Cèze, France
[c] The Rossendorf Beamline at the ESRF, CS40220, 38043 Grenoble Cedex 9, France.
[d] Helmholtz Zentrum Dresden-Rossendorf (HZDR), Institute of Resource Ecology, P.O. Box 510119, 01314, Dresden, Germany.
[e] Synchrotron SOLEIL L'Orme des Merisiers, Saint-Aubin, BP 48, F-91192 Gif-sur-Yvette Cedex France
*N. D.: phone. +33 4 66 33 92 05; e-mail. nicolas.dacheux@umontpellier.fr
*T. D.: phone. + 33 4 66 79 65 87: e-mail. thomas.dumas@cea.fr
Electronic Supplementary Information (ESI) available: See DOI: 10.1039/x0xx00000x

due to their low isoelectric point (pH_{IEP}(Th) = 4.6,[2] pH_{IEP}(U) = 4.4 [3] and pH_{IEP}(Np) = 2.6 [4, 24] against pH_{IEP} close to 8 for the respective actinide oxy-hydroxides colloids [24]).

Table 1. Conditions reported for the formation of actinide (IV) silicate colloids in carbonate ions rich reactive media and in carbonate ions free reactive media, where their formation was suspected (after ultrafiltration of the corresponding solutions).

Observation in carbonate ions rich reactive media					
Reference	Actinide-silicate system	Conditions	pH	Colloids size	
				Below MWSA	Above MWSA
[2]	Th-silicate	$[NaHCO_3] = 0.05$ mol·L^{-1} $[Th] = 10^{-3}$ mol·L^{-1} Si/Th = 0.3 – 8	≥ 7	7 – 20 nm	
[3, 22]	U-silicate	$[NaHCO_3] = 0.05$ mol·L^{-1} $[U] = 10^{-3}$ mol·L^{-1} Si/U = 0.25 – 3	7 – 9.5	≤ 20 nm	
[23]	U-silicate	$[NaHCO_3] = 0.05$ mol·L^{-1} $[U] = 10^{-3}$ mol·L^{-1} Si/U = 2 – 4	9 – 10.5	1 – 10 nm	≤ 220 nm
[4, 24]	Np-silicate	$[NaHCO_3] = 0.1$ mol·L^{-1} $[Np] = 10^{-3}$ mol·L^{-1} Si/Np = 0.7 – 8.6	7 – 9	5 nm	≤ 250 nm
Observation in carbonate ions free reactive media					
Reference	Actinide-silicate system	Conditions	pH	Colloids size	
				Below MWSA	Above MWSA
[19]	Th-silicate	$ThO_2 \cdot xH_2O$ $[Si] = 10^{-3} – 0.15$ mol·L^{-1}	6 – 12	Th solubility increase	6 – 12
[17]	Th-silicate	$ThO_2 \cdot xH_2O$ $[Si] = 1.8 \times 10^{-2}$ mol·L^{-1}	10 – 13.3	Th solubility increase	10 – 13.3
[14]	Pu-silicate	$PuO_2 \cdot xH_2O$ $[Si] = 10^{-3} – 10^{-2}$ mol·L^{-1}	11 – 13.8	Pu solubility increase	11 – 13.8

MWSA : Mononuclear wall of silicic acid

These colloids correspond to 1 – 20 nm particles at low silicate ions concentrations (below silicic acid mononuclear wall; [Si] = 2×10^{-3} mol·L^{-1} [25]) and ~ 200 nm agglomerates at higher concentrations. Moreover, structural characterizations performed by EXAFS spectroscopy [2-4, 20-22, 24] allowed to observe that the actinide coordination shell in these silicate colloids was analogous to the one determined for solid actinide (IV) silicates, $AnSiO_4$, (zircon type structure).[26] However, even if the formation of actinide silicate colloids has been clearly identified in carbonate ions rich reactive media, the formation of these species in carbonate ions free reactive media has been only suspected for thorium in alkaline conditions and may also be suspected for plutonium (**Table 1**). [2-4, 14, 17, 19, 22-24]

In this work, the experiments were focused on the chemistry of Pu(IV) in very alkaline silicate ions reactive media, in order to provide an explanation on the increase of plutonium solubility reported in the literature. However, unlike the previous literature's experiments, we chose to work in nearly saturated silicate ions reactive media, in order to facilitate the identification of the potential Pu(IV)-silicate species obtained in these conditions.

Materials and methods

Samples preparation

Caution! ^{238}Pu, ^{239}Pu, ^{240}Pu and ^{242}Pu are α-emitter and ^{241}Pu is β$^-$-emitter which are considered as a health risk. Experiments involving actinides require appropriate facilities and trained persons in handling of radioactive materials.

Experiments were performed into glove box at the ATALANTE Facility of Marcoule Research Centre, France. The stock solution of plutonium (isotope mixture: 0.04% ^{238}Pu, 95.77% ^{239}Pu, 3.70% ^{240}Pu, 0.14% ^{241}Pu, 0.35% ^{242}Pu) was purified by a standard anion-exchange method, in order to remove ^{241}Am produced by β-decay of ^{241}Pu product.[27] Plutonium was stabilized in the oxidation state +IV, in a 1.5 mol·L^{-1} HNO_3 solution. It was then titrated by UV-visible spectroscopic method, by standard deconvolution from reference measurements ($C_{Pu} = 0.30 \pm 0.03$ mol·L^{-1}).

An aqueous silicate solution was prepared by dissolving $Na_2SiO_3 \cdot 9H_2O$ (98%) supplied by Sigma-Aldrich in water in order to obtain a nearly saturated aqueous solution ($C_{Na2SiO3} \approx 2$ mol·L^{-1}). Experiments were performed by adding of the Pu(IV) stock solution to 0.8 mL of the silicate solution under vigorous stirring (500 rpm). Then, the pH of the reactive media was controlled. The precipitates obtained were separated from the supernatant by centrifugation for 14 min

at 14,000 rpm, corresponding to a cut-off of size around 150 nm according to the calculation method described by Livshts *et al.*[28]. UV-visible and XAS measurements were performed on the as-obtained supernatant.

In order to evaluate the size of the colloids, additional experiments were performed from the raw aqueous solutions which were centrifugated for 10 min à 4,500 rpm (corresponding to a cut-off of size around 550 nm)[28], in order to eliminate the largest precipitated particles. The solution was then filtrated thanks to Whatman® Anotop 0.45 µm, 0.1 µm and 0.02 µm syringe filters and ultrafiltrated thanks Merck® Amicon Ultra to 100 kDa, 10 kDa and 3 kDa filters units (i.e. pores diameters 6.1 nm, 2.9 nm and 2.0 nm, respectively)[15]. Aliquots were taken at each filtration step in order to measure the concentration of plutonium thanks to α counting measurements and to perform additional characterizations.

Characterization

All of the UV-visible spectrophotometric measurements were performed on a Varian Cary 6000i spectrophotometer installed outside of the glove box with a fiber-optic signal transmission line. Measurements were performed in quartz cells between λ = 350 nm and 900 nm. Due to the specific analysis conditions with long glass fibers between the spectrometer and the sample located in a glovebox. Therefore, deconvolutions of the spectra were performed using reference spectra of actinide solutions with known concentrations previously recorded in the same conditions.

The Extended X-ray Absorption Fine Structure (EXAFS) and X-Ray Absorption Near Edge Structure (XANES) spectroscopy measurements were carried out at the MARS beamline at the SOLEIL synchrotron facility (Saint-Aubin).[29] The spectra were collected in the fluorescence mode with a 13 element Ge detector at ambient temperature. Measurements have been performed at the plutonium L_{III} edge (18057 eV). Data reduction and extraction of EXAFS oscillation was performed using the Athena and Artemis package.[30] The threshold energy, E_0, was defined as the maximum of the first derivate of the absorption coefficient. Experimental EXAFS spectra were Fourier Transformed (FT) using a Hanning window over the k-space range 2−11 $Å^{-1}$. The shell fits were performed in R-space on the k^3 weighted FT EXAFS oscillations. Theoretical phase shifts and backscattering amplitudes were obtained with the ab initio code FEFF8.2 [31] using the reference $PuSiO_4$ and $CeSiO_4$ structures.[7, 32]

The concentration of Pu in colloidal solutions was determined by α-spectrometry (7401 Canberra) performed at the energy of ^{239}Pu α-decay. The spectrometer was calibrated with sealed sources samples with known activities. Prior the measurement, the samples were diluted and a determined volume was deposited on a stainless steel sample holder and then evaporated by heating.

pH determinations were performed with a Metrohm pH electrode, allowing pH measurement on the 0-14 pH range, calibrated thanks to pH = 2.00, 7.00 and 12.45 buffer solutions.

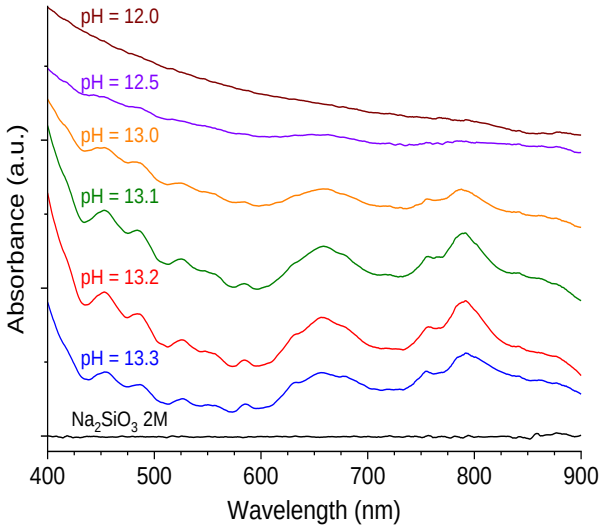

Fig 1. UV-visible spectra of Pu(IV) in a 2 mol·L^{-1} Na_2SiO_3 solution depending on the pH of the reactive media (i.e. on the amount of the mother solution of Pu(IV) in HNO_3 1 mol·L^{-1} added gathered in **Table S1**).

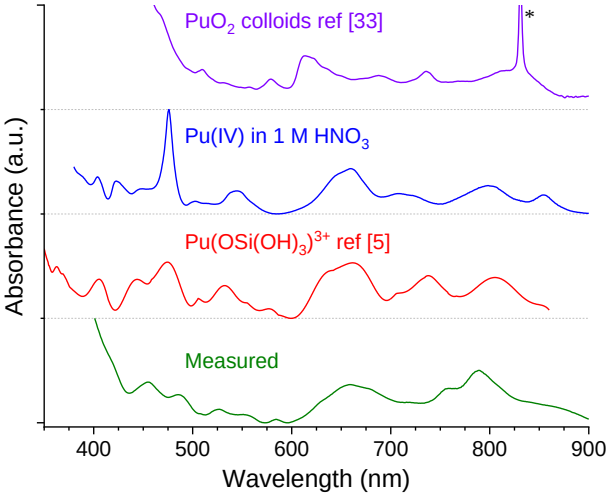

Fig 2. UV-visible spectrum of a Pu(IV)-silicate solution (pH = 13.2, $C_{Na2SiO3} \approx 2$ mol·L^{-1}, $C_{Pu} = 3 \times 10^{-2}$ mol·L^{-1}), compared with the spectra reported by Dalodière *et al.*[33] for Pu(IV) colloidal solution (PuO_2^{2+} observed as impurities at λ = 830 nm, identified by an asterisk), with that of a Pu(IV) solution prepared in 1 mol·L^{-1} HNO_3) and that of the $Pu(OSi(OH)_3)^{3+}$ complex reported by Yusov *et al.*[5].

Results and discussion

Preparation of a nearly saturated Na_2SiO_3 solution led to the very alkaline aqueous reactive media (pH ≈ 13.3). Successive addition of the mother Pu(IV) solution in nitric acid media to this Na_2SiO_3 solution led to a pH decrease (**Table S1** and **Figure S1**) and allowed to observe the formation of aqueous plutonium species for pH ≥ 13 (**Figure 1**), characterized by the absorption bands observed at λ = 455, 486, 526, 551, 584, 633, 654, 677, 755 and 793 nm. The as-obtained alkaline plutonium silicates were green-colored solutions and remained stable for months (**Figure S2**). Decreasing the pH of the reactive media led to gelation for pH ≤ 13 and a strong decrease of the

plutonium solubility. Measurements performed at pH ≤ 12 did not allow the identification of aqueous plutonium species. This observation could be explained by silicate ions protonation, considering $HSiO_3^-/SiO_3^{2-}$ or $H_3SiO_4^-/H_2SiO_4^{2-}$ acid constants. The associated constant values were evaluated to $pK_a = 11.99$ [34] and $pK_a = 13.30$,[35] respectively. This would drastically change the chemical conditions in the reactive media, modify the silicate species solubility and thus the gelation conditions in the reactive media. Moreover, it might be inferred that protonated silicate based species (e.g. $H_3SiO_4^-$) would present a lower affinity regarding to plutonium compared to SiO_3^{2-} / $H_2SiO_4^{2-}$ ions.

The comparison with aqueous plutonium oxo-hydroxo colloids solution allowed to observe that the as-obtained plutonium species did not correspond to hydrolyzed plutonium (**Figure 2**) nor to the plutonium silicate complex, $PuOSi(OH)_3^{3+}$, reported by Pazukhin *et al.*[6] and Yusov *et al.*[5] but might correspond to aqueous plutonium silicate species, such as $Pu(SiO_3)_n^{(4-2n)}$ proposed by Shilov and Fedoseev [14] however, to the best of our knowledge, no UV-visible spectra of that specie was reported. Putting an aliquot of alkaline plutonium silicate in 1 mol·L^{-1} HNO_3 led to the full dissociation of the silicate species, evidenced by the obtention of UV-vis spectra characteristic of Pu(IV) in 1 M nitric acid. The solution was characterized a few minutes after the acidification and no change of the corresponding UV-vis spectra was observed over time, corresponding to a fast dissociation process, corresponding to a very different behavior from that of the nearly insoluble plutonium oxo-hydroxy colloids. This protocol allowed to determine the Pu concentration in solution using UV-vis spectrophotometry. In the Pu silicate solution at pH = 13.2, the highest Pu concentration measured was $C_{Pu} = 3 \times 10^{-2}$ mol·L^{-1}, however, the formation of colloids seems to be very sensitive to the experimental conditions and most of the measurement on these solutions led to concentration around 10^{-2} mol·L^{-1} (**Figure S1**).

Filtration experiments have been performed on the plutonium silicate colloidal solution to check if the obtained species corresponding to complexes or colloidal particles. A sequential filtration process was performed on the raw solution centrifuged during 10 min at 4,500 rpm (cut off of size around 550 nm)[28] then filtered at 0.45 µm, 0.1 µm, 0.02 µm, 100 kDa (6.1 nm)[15], 10 kDa (2.9 nm)[15] and 3 kDa (2.0 nm)[15]. The plutonium concentration after filtration was measured by α spectrometry (**Figure 3a** and **Table 2**). It was measured around $(12 \pm 2) \times 10^{-3}$ mol·L^{-1} for the sample filtered at 0.45 µm and decreased down to $(8.4 \pm 0.8) \times 10^{-3}$ mol·L^{-1} to reach a plateau for filtration steps at 0.1 µm, 0.02 µm, 100 kDa. This first decrease could be assigned to the elimination of the largest particles present in solution. It allowed discriminating the size of the plutonium silicate species measured to be below 6.1 nm [15]. It is worth noting that the particle agglomeration, which has been generally described for actinide silicate colloids formed above the silicic acid mononuclear wall, [4, 23, 24] was not observed in that case. It might be explained by the very alkaline conditions considered leading to nanoparticles with negative surface charge which could have minimized the agglomeration tendency due to electrostatic repulsion. The concentration obtained for the filtration at 10 kDa and 3 kDa were measured to $(2.7 \pm 0.3) \times 10^{-3}$ mol·L^{-1} and $(1.7 \pm 0.3) \times 10^{-3}$ mol·L^{-1}. These results demonstrated that the particles observed were in the colloidal form with a quite homogeneous size distribution and a median size ranging from 6.1 nm to 2.9 nm.[15] This size is consistent with that obtained for PuO_2 nanoparticles (i.e. 2 to 3 nm).[33, 36-39] The plutonium concentration after filtrations at 10 kDa and 3 kDa remained quite high for such alkaline plutonium aqueous solutions. This result might be explained by different hypotheses: the presence of very small Pu-silicate colloidal particles, solution leaks or membrane breaks of the filter units which could have

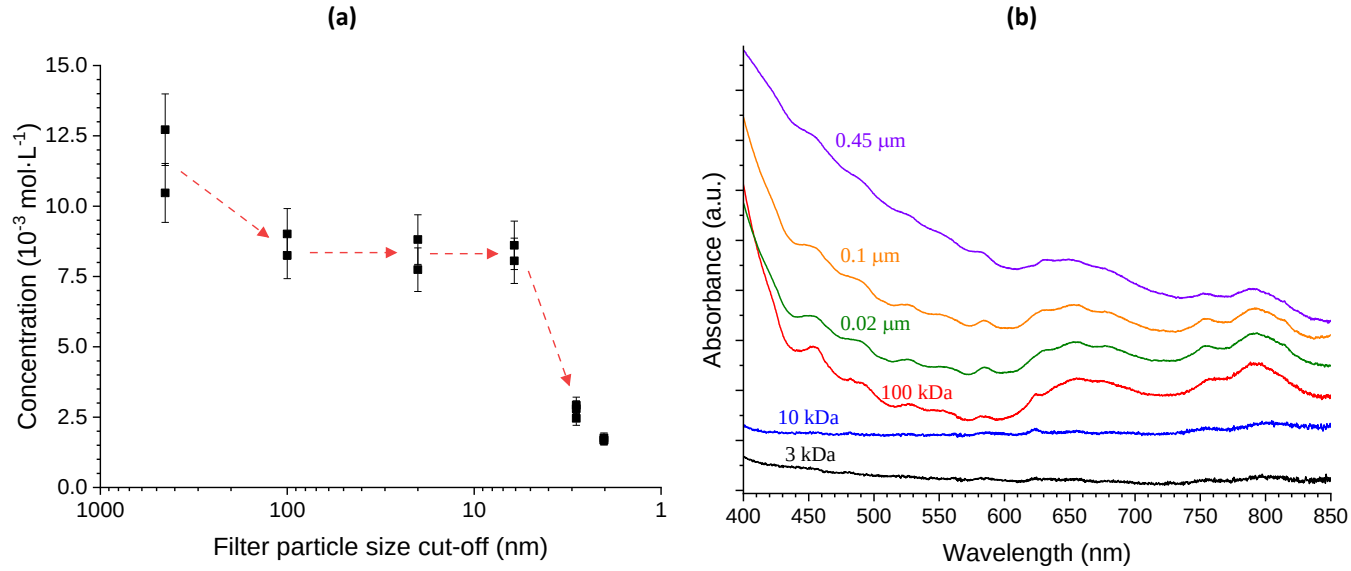

Fig 3. Pu(IV)-silicate solution (pH = 13.2, $C_{Na2SiO3} \approx 2$ mol·L^{-1}) concentration determined by alpha spectrometry (a) and UV-visible spectra (b) for solutions filtrated at 0.45 µm, 0.1 µm, 0.02 µm, 100 kDa, 10 kDa and 3 kDa. The red arrows in Fig 3.a were added only to make the results easier to read.

allowed the partial diffusion of plutonium species or the formation of Pu-silicate complexes. This last hypothesis might be compared to the formation of $[Th(OH)_3(OSi(OH)_3)_3]^{2-}$ complexes which has been suggested in literature for thorium in silicate rich and alkaline media.[17] However, it was not clearly evidenced for plutonium in this study.

Table 2. Pu(IV)-silicate solution (pH = 13.2, $C_{Na2SiO3} \approx 2$ mol·L^{-1}) concentration determined by alpha spectrometry for solutions filtrated at 0.45 µm, 0.1 µm, 0.02 µm, 100 kDa, 10 kDa and 3 kDa.

Filter cut-off	Measured concentrations (× 10^{-3} mol·L^{-1})*		
0.45 µm	10.4	12.7	---
0.1 µm	8.25	9.01	---
0.02 µm	7.74	8.81	---
100 kDa (6.1 nm)	8.61	8.06	---
10 kDa (2.9 nm)	2.92	2.80	2.46
3 kDa (2.0 nm)	1.76	1.69	1.68

* Measurement uncertainty: 10%

Additionally, UV-vis spectra were measured on the filtered solution aiming at verifying the nature of the species obtained (**Figure 3b**). For the filtration above 100 kDa, the spectra have been found to be similar to the ones previously reported (**Figure 1** and **Figure 2**). The statement on the elimination of the largest suspended nanoparticles, between the filtration steps at 0.45 µm and 0.1 µm, was confirmed by UV-vis spectroscopy, with the decrease of the background absorbance at $\lambda < 600$ nm which could be attributed to Mie scattering. According to the results expected by Beer Lambert law, nearly no additional difference was observed between the supernatants obtained after filtration at 0.1 µm, 0.02 µm and 100 kDa. Indeed, the only slight modification observed could be due to the elimination of SiO_2 colloids. However, one other strong decrease in intensity was observed when performing the filtration at 10 kDa or at 3 kDa. All of these results are in good agreement with a particle size distribution with a median size ranging from 6.1 nm to 2.9 nm.

In order to determine the structure of these plutonium silicate colloids, XAS measurements were performed at plutonium L_{III} edge on unfiltered samples (after centrifugation). First, the XANES spectrum carried out on this sample enabled the identification of Pu(IV) as the predominant oxidation state, from its characteristic maximum absorption peak at 18068 eV and because of the absence of the shoulder feature at 18082 eV typical of Pu(V) or Pu(VI) (**Figure 4**), confirming the tetravalent oxidation state of plutonium in the considered silicate species.

Secondarily, the plutonium coordination sphere was studied using the pseudo-radial distribution function obtained from the Fourier Transform of the EXAFS oscillations (**Figure 5**). From the EXAFS spectrum and corresponding FT, it was already possible to exclude the formation of intrinsic plutonium oxy-hydroxide colloids by comparison with previously reported EXAFS spectra.[33, 40, 41] The obtained spectra exhibited similarities with the actinide silicate colloids already identified for thorium(IV), uranium(IV) and neptunium(IV).[2-4, 23] For these three actinide silicate systems, three main scattering shells were distinguished on the Fourier Transform: a first peak at $R + \Delta = 1.6$ Å attributed to the An(IV)-Oxygen interactions, the second shell at $2.3 \text{ Å} \leq R + \Delta \leq 3.2$ Å attributed to A(IV)-Si interactions and for $3.0 \text{ Å} \leq R + \Delta \leq 4.0$ Å, An(IV)-An(IV) interactions were evidenced. This suggests structural similarities between these colloids and the aqueous plutonium silicate species obtained in this work. Therefore, the model used for the analysis of the EXAFS measurement was based on the data treatment performed for each of these actinide silicate colloids. Consequently, the structure was derived from those reported in the literature for tetravalent actinide silicates, $AnSiO_4$ (**Table S2**). Because $PuSiO_4$ and $CeSiO_4$ are reported to be isostructural [7, 32] and octacoordinated, Pu^{4+} and Ce^{4+} exhibit close ionic radii ($r(^{VIII}Pu^{4+}) = 0.96$ Å ; $r(^{VIII}Ce^{4+}) = 0.97$ Å),[42] the atomic positions of oxygen, which are not reported in the $PuSiO_4$ structure, were considered to be similar to those reported for $CeSiO_4$. In the model used for the fit of the EXAFS spectra, coordination numbers, interatomic distances and Debye-Waller factors were taken as adjustment variables. However, since the structure of the measured species is very disordered and too much free parameters did not allowed the model to merge to reasonable values, the number of oxygen atoms were fixed and the Debye Waller

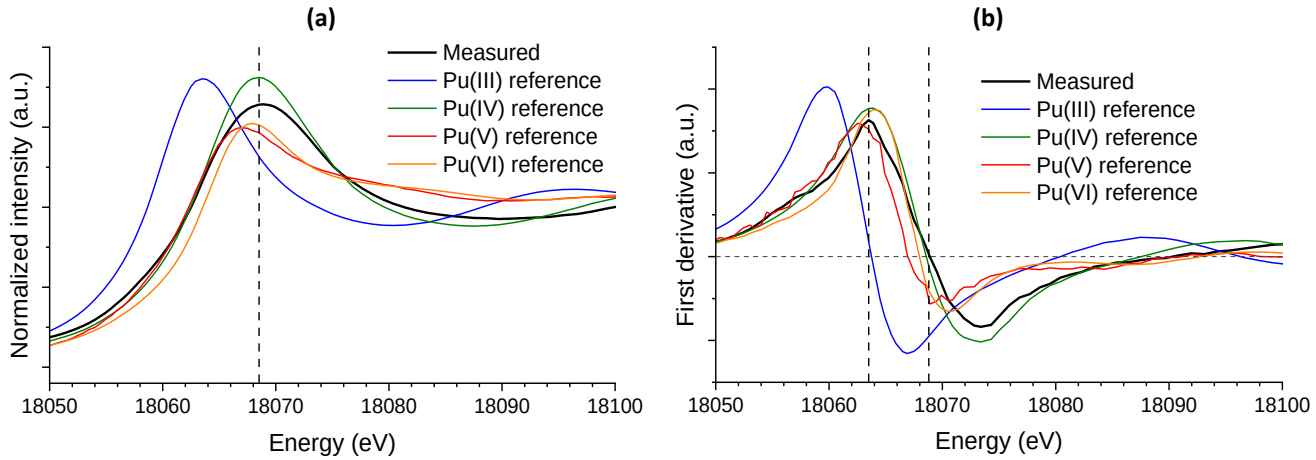

Fig 4. XANES spectra (a) and respective first derivative (b) at plutonium L_{III} edge for a Pu(IV)-silicate solution with $C_{Na2SiO3} = 2$ mol·L^{-1}, $C_{Pu} \approx 10^{-2}$ mol·L^{-1} and pH = 13.2.

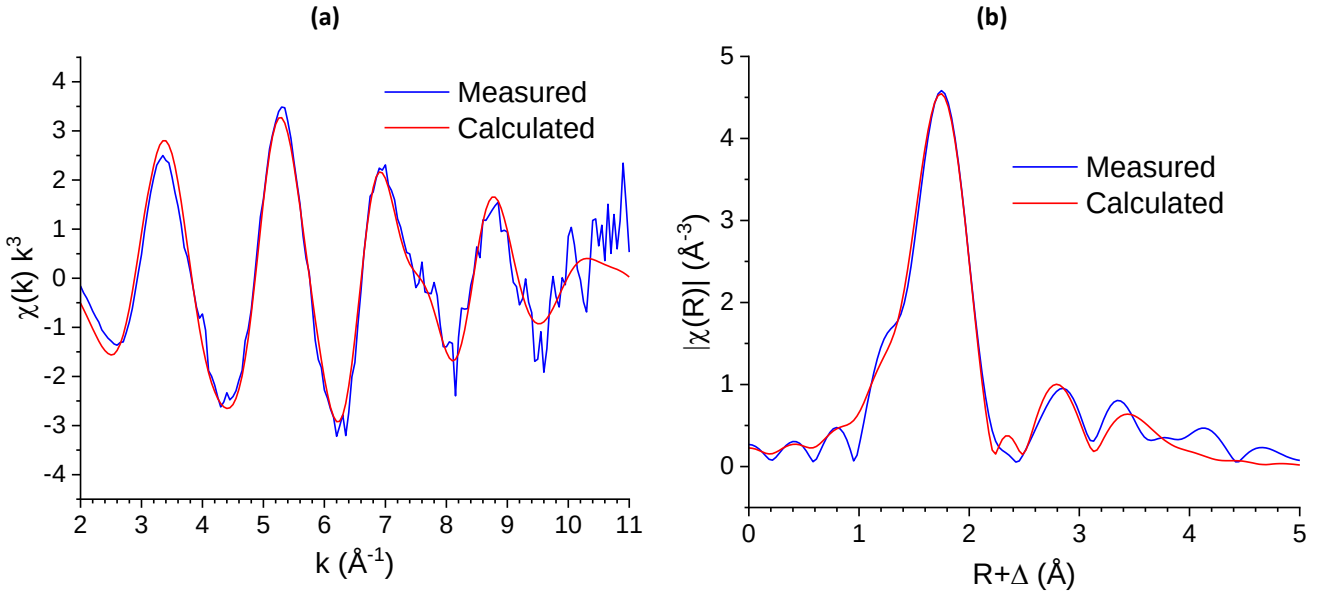

Fig 5. EXAFS spectra 2 Å < k < 11 Å (a) and respective Fourier Transform (b) at plutonium L_{III} edge for a Pu(IV)-silicate solution with $C_{Na2SiO3}$ = 2 mol·L^{-1}, $C_{Pu} \approx 10^{-2}$ mol·L^{-1} and pH = 13.2.

parameters for Pu-Si were chosen to be in the same range as the value reported in the literature for the An-silicate colloids (**Table S3**).

The first peak and its shoulder obtained for the pseudo-radial distribution function were hence attributed to oxygen atoms in the first coordination sphere of plutonium, R(Pu-O_1) = 2.23(2) Å and R(Pu-O_2) = 2.34(3) Å (**Figure 5** and **Table 3**) in good agreement with the values reported in the literature for R(An-O) (i.e. 2.2 – 2.5 Å) (**Table S3**). The two next peaks have been attributed to silicon atoms in the second coordination sphere of plutonium and correspond to the presence of bidentate and monodentate silicate groups. Consistently with previous hypotheses from Hennig *et al.*[2], Neill *et al.*[23] and Husar *et al.*[4], bidentate silicate groups correspond to shorter Pu-Si distances (R(Pu-Si_1) = 3.21(6) Å) than monodentate groups (R(Pu-Si_2) = 3.46(3) Å). The resulting coordination numbers for silicates show more monodentate groups and less bidentate groups than that was expected (CN(Pu-Si_2) = 5.4(22) and CN(Pu-Si_1) = 1.1(9) against CN(Pu-Si_2) = 4 and CN(Pu-Si_1) = 2) and might indicate a disordered structure. At further distance, a third contribution may be assigned to the plutonium-plutonium interactions. The quite low intensity of this contribution, CN(Pu-Pu) = 6.0(21), and the high Debye Waller parameter associated (σ^2(Pu-Pu) = 0.020(26) Å^2) indicate that the long-range structure is disordered. All of these results, on both the interatomic distance measured and the structural disorder, are consistent with the results already reported for An(IV)-silicate colloids, with An = Th, U and Np (**Table 4**). Moreover, considering the distances reported for the solid $CeSiO_4$ and $USiO_4$ and extrapolated for $PuSiO_4$, the Pu-Si and Pu-Pu distances are in good agreement with the formation of a tetravalent plutonium silicate compound (**Table 3**). These observations support the previous hypothesis of the formation of amorphous An(IV) silicate particles in which the local structure of plutonium is a disordered An(IV) silicate-like structure.

Table 3. Structural parameters determined for Pu(IV)-silicate species ($C_{Na2SiO3}$ = 2 mol·L^{-1}, $C_{Pu} \approx 10^{-2}$ mol·L^{-1} and pH = 13.2) and expected interatomic distances for $PuSiO_4$.[7] The values fixed for the simulations have been marked by an asterisk. $\Delta E_{k=0}$ = – 1.4 eV, F = 0.07, S_0^2 = 0.9.

	R (Å)	N	σ^2 (Å^2)	Expected R (Å) for $PuSiO_4$
Pu-O_1	2.23 (2)	4 *	0.007 (3)	---
Pu-O_2	2.34 (3)	4 *	0.007 (3)	---
Pu-Si_1	3.21 (6)	1.1 (9)	0.009*	3.11
Pu-Si_2	3.46 (3)	5.4 (22)	0.012*	3.79
Pu-Pu	3.77 (3)	6.0 (21)	0.020 (26)	3.79

Table 4. Structural parameters determined for Pu(IV)-silicate species ($C_{Na2SiO3}$ = 2 mol·L^{-1}, $C_{Pu} \approx 10^{-2}$ mol·L^{-1} and pH = 13.2) and reported in the literature for An(IV)-silicate colloids. Uncertainties were omitted for clarity; all of the data are available in Table S3.

An	Th [2]	U [22]	U [23]	Np [2]	Pu (this study)
An-O_1	R = 2.36–2.39 Å *N = 8.3–8.9*	R = 2.23–2.25 Å *N = 2.7–4.1*	R = 2.23–2.30 Å N = *3.7–4.7*	R = 2.28 Å *N = 7.1*	R = 2.23 Å *N = 4*
An-O_2			R = 2.44–2.47 Å *N = 3.0–3.9*		R = 2.34 Å *N = 4*
An-Si_1	R = 3.23–3.26 Å *N = 1.3–2.5*	R = 2.81–2.83 Å *N = 2.7–3.5*	R = 3.17–3.19 Å *N = 0.9–1.6*	R = 3.11 Å *N = 1.3*	R = 3.21 Å *N = 1.1*
An-Si_2			R = 3.70–3.76 Å *N = 0.8–2.5*		R = 3.46 Å *N = 5.4*
An-An	---	R = 3.85 Å *N = 2.6*	R = 3.78–3.86 Å *N = 1.0–5.0*	R = 3.75 Å *N = 1.1*	R = 3.77 Å *N = 6.0*

Therefore, the plutonium species obtained in silicate ions rich and very alkaline reactive media may be attributed to the formation of plutonium silicate-based colloids close to those reported for the other actinide silicate colloids (**Table S3**) with a short-distance environment similar to the one expected for $PuSiO_4$. The small size of the colloidal particles, range from 2.9 to 6.1 nm for Pu-Pu distances measured at 0.377 nm, might also explain the strong disorder observed in EXAFS, because of the over-representation of the plutonium located on the surface of the nanoparticles compared to the ones located in the core of the colloids (roughly representing 30-60% of the Pu atoms for that size of nanoparticles).

Moreover, in order to describe the nature of the samples and to rule out any important change on aged and filtered samples, EXAFS spectra have been recorded on the solutions filtered at 0.45 µm and 100 kDa and the one-year aged system filtered at 100 kDa prior the ageing. The k^3 weighted spectra and corresponding Fourier Transforms as well as the best fit parameters are presented in **Figure 6** and **Table S3**. Overall, the EXAFS signal does not exhibit noticeable differences considering uncertainties and the plutonium silicate colloids structure is unaltered. Indeed, the main Pu-O contributions, as well as second sphere Pu-Si and Pu-Pu contributions, are still present. Consequently, the plutonium species observed could clearly be identified as plutonium (IV) bearing silicate colloids and it has been evidenced that these colloidal suspensions were stable over time.

Conclusions

Studying the speciation of Pu(IV) in very alkaline and silicate ions rich reactive media allowed identifying the formation of plutonium (IV)-silicate colloidal suspensions which were stable for months. Their structural characterization evidenced that their structure was very similar to those identified for the other actinide-silicate colloidal systems.[2, 18-21] These colloids were smaller than 6 nm in size, which was very close to that usually observed for PuO_2 nanoparticles,[33, 37, 38] probably leading to comparable properties in terms of mobility. The conditions tested allowed stabilizing colloidal suspensions for Pu(IV) concentration around 10^{-2} mol·L^{-1} and pH values up to 13 in silicate ions reactive media.

Based on these observations, the solubility increase observed for plutonium in alkaline silica solutions [14, 17] might be explained by the formation of such silicate colloids, which

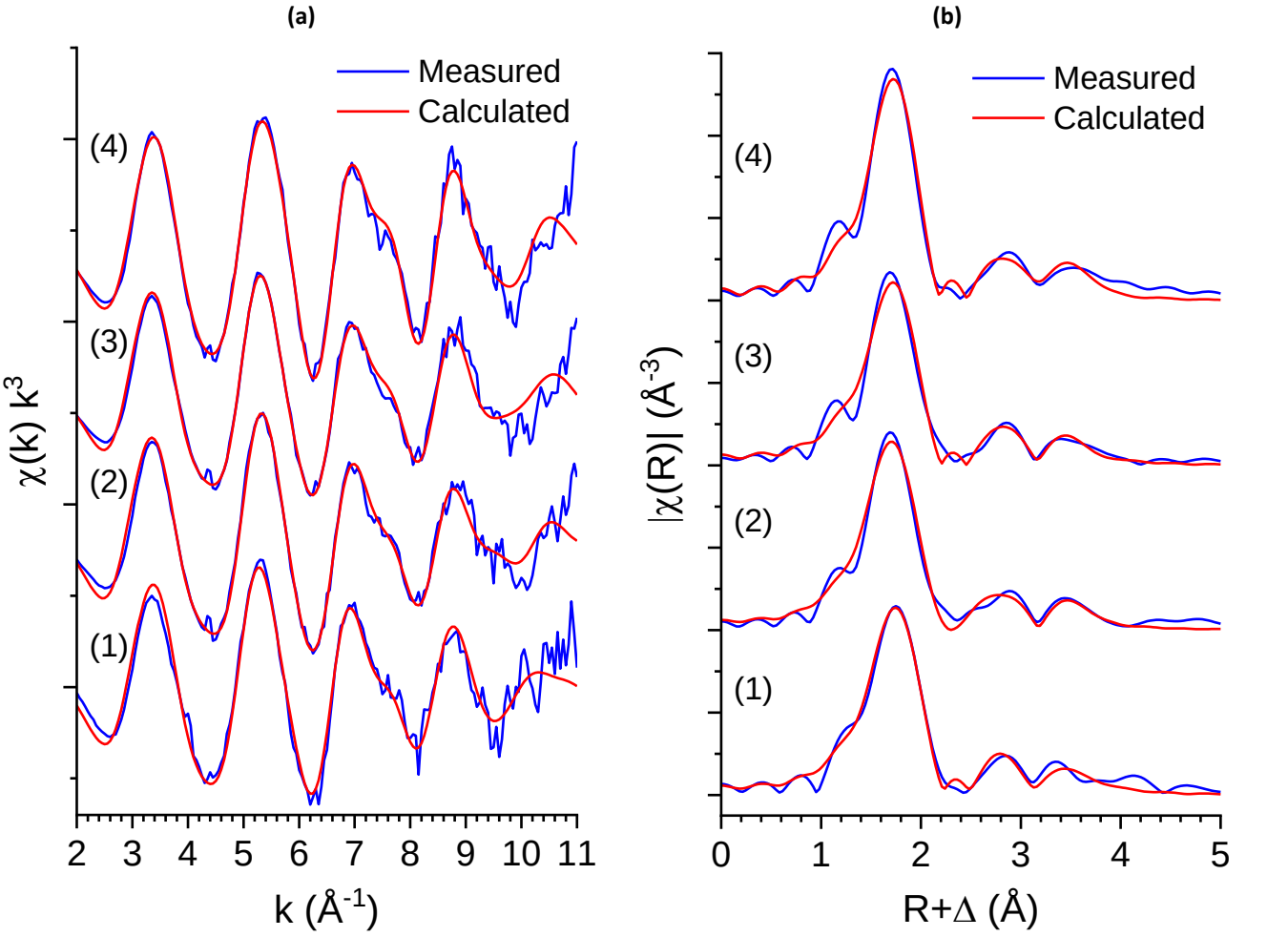

Fig 6. EXAFS spectra 2 Å < k < 11 Å (a) and respective Fourier Transform (b) at plutonium L_{III} edge for the Pu(IV)-silicate colloids solution for the reference sample (1), a sample filtered at 0.45 µm (2), a sample filtered at 100 kDa (3) and a sample filtered at 100 kDa 1 year-old aged (4).

could affect the plutonium mobility. Specifically, it may partially explain the plutonium mobility in some contaminated sites, such as Mortandad Canyon,[43, 44] Savannah River,[45] the Nevada Test Site [46] or the Mayak production association.[47] Moreover, the formation of actinide bearing silicate colloids has to be considered in the field of high level radioactive waste disposal, especially in permeable media. In this context, the identification of plutonium (IV)-silicate interactions constitutes one of the first steps for a better understanding of plutonium environmental chemistry.

Supporting information

Table S1 reporting the results of the UV-visible and pH monitoring of the solution resulting from the addition of Pu(IV) nitric solution in Na_2SiO_3 2 mol·L^{-1} aqueous solution. **Table S2** gathering interatomic distances reported for $ThSiO_4$, $USiO_4$, $CeSiO_4$ and $PuSiO_4$.[7, 32, 48, 49] **Table S3** reporting the structural parameters determined by EXAFS characterization for the actinide silicate colloids.[2, 22-24] **Figure S1** representing the pH monitoring of Na_2SiO_3 2 mol·L^{-1} aqueous solution depending on the addition of Pu(IV) nitric solution. **Figure S2** representing the UV-visible spectra of a Pu(IV)-silicate solution freshly prepared and after a 3 months ageing. **Figure S3** reporting the picture of the Pu-silicate colloids solution filtrated at 0.1 µm and 3 kDa. **Figure S4** representing the EXAFS spectra and the respective FT of the Pu-silicate colloids solution filtrated at 0.45 µm. **Figure S5** representing the EXAFS spectra and the respective FT of the Pu-silicate colloids solution filtrated at 100 kDa. **Figure S6** representing the EXAFS spectra and the respective FT of the Pu-silicate colloids solution filtrated at 100 kDa and one year old aged. This material is available free of charge via the Internet at http://pubs.acs.org.

Conflicts of interest

There are no conflicts to declare.

Acknowledgements

This research was funded by The French Alternative Energies and Atomic Energy Commission and the European Commission Council under ERC, under grant agreement 759696.
The authors would like to thank V. Brethenoux, J. Hennuyer, J. Vermeulen and E. Russello (from CEA) for supporting the experiments.

Notes and references

1. E. Gonzales, B. C. Na, M. Salvatores, C. H. Zimmerman, F. Varaine, A. D'Angelo, M. Schikorr, J. C. Kuijper, P. Coddington and Y. H. Kim, *Physics and safety of transmutation systems - A status report*, Nuclear Energy Agency, 2006.
2. C. Hennig, S. Weiss, D. Banerjee, E. Brendler, V. Honkimäki, G. Cuello, A. Ikeda-Ohno, A. C. Scheinost and H. Zänker, *Geochimica et Cosmochimica Acta*, 2013, **103**, 197-212.
3. I. Dreissig, S. Weiss, C. Hennig, G. Bernhard and H. Zänker, *Geochimica et Cosmochimica Acta*, 2011, **75**, 352-367.
4. R. Husar, S. Weiss, C. Hennig, R. Hübner, A. Ikeda-ohno and H. Zänker, *Environmental Science & Technology*, 2015, **49**, 665-671.
5. A. B. Yusov, A. M. Fedosseev and C. H. Delegard, *Radiochimica Acta*, 2004, **92**, 869-881.
6. E. M. Pazukhin, A. S. Krivokhatskii and E. G. Kudryatsev, *Soviet Radiochemistry*, 1990, **32**, 26-32.
7. C. Keller, *Nukleonik*, 1963, **5**, 41-48.
8. A. Mesbah, S. Szenknect, N. Clavier, J. Lozano-Rodriguez, C. Poinssot, C. Den Auwer, R. C. Ewing and N. Dacheux, *Inorganic Chemistry*, 2015, **54**, 6687-6696.
9. P. Estevenon, T. Kaczmarek, F. Vadot, T. Dumas, P. L. Solari, E. Welcomme, S. Szenknect, A. Mesbah, P. Moisy, C. Poinssot and N. Dacheux, *Dalton Transactions*, 2019, **48**, 10455-10463.
10. P. Estevenon, E. Welcomme, C. Tamain, G. Jouan, S. Szenknect, A. Mesbah, C. Poinssot, P. Moisy and N. Dacheux, *Dalton Transactions*, 2020, **49**, 6434 - 6445.
11. P. Estevenon, E. Welcomme, J. Causse, S. Szenknect, A. Mesbah, P. Moisy, C. Poinssot and N. Dacheux, *Dalton Transactions*, 2020, **49**, 11512-11521
12. P. Estevenon, E. Welcomme, S. Szenknect, A. Mesbah, P. Moisy, C. Poinssot and N. Dacheux, *Dalton Transactions*, 2019, **48**, 7551-7559.
13. V. Neck and J. I. Kim, *Radiochimica Acta*, 2001, **89**, 1-16.
14. V. P. Shilov and A. M. Fedoseev, *Radiokhimiya*, 2003, **45**, 491-494.
15. H. P. Erickson, *Biological Procedures Online*, 2009, **15**, 32-51.
16. M. P. Jensen, Ph.D. Thesis. Florida State University, 1994.
17. D. Rai, M. Yui, D. A. Moore, G. J. Lumetta, K. M. Rosso, Y. Xia, A. R. Felmy and F. N. Skomurski, *Journal of Solution Chemistry*, 2008, **37**, 1725-1746.
18. C. Riglet-Martial, I. Laszak, L. Bion and P. Vitorge, *Competition carbonate-silicate sur la complexation des actinides en milieu argileux riche en silice*, CEA, 2000.
19. V. Peretroukhine, C. Riglet-Martial, H. Capdevila, V. Calmon, P. Bienvenu and I. Laszak, *Journal of Nuclear Science and Technology*, 2002, **Supplement**, 516-519.
20. H. Zänker and C. Hennig, *Journal of Contaminant Hydrology*, 2014, **157**, 87-105.
21. H. Zänker, S. Weiss, C. Hennig, V. Brendler and A. Ikeda-Ohno, *Chemistry Open*, 2016, **5**, 174-182.
22. I. Ulbricht, Ph.D. Thesis. Technischen Universität Dresden, 2010.
23. T. S. Neill, K. Morris, C. I. Pearce, N. K. Sherriff, M. G. Burke, P. A. Chater, A. Janssen, L. S. Natrajan and S. Shaw, *Environmental Science & Technology*, 2018, **52**, 9118–9127.
24. R. Husar, Ph.D. Thesis. Technischen Universität Dresden, 2015.
25. W. Stumm, H. Hüper and L. Champlin, *Environmental Science and Technology*, 1967, **1**, 221-227.
26. J. A. Speer, *Reviews in Mineralogy and Geochemistry*, 1980, **5**, 113-135.
27. A. Kaya, H. Kud, J. Shirahashi and S. Suzuki, *Journal of Nuclear Science and Technology*, 1967, **4**, 289-292.

28. M. A. Livshts, E. Khomyakova, E. G. Evtushenko, V. N. Lazarev, N. A. Kulemin, S. E. Semina, E. V. Generozov and V. M. Govorun, *Scientific Reports*, 2015, **5**, 17319.
29. I. Llorens, P. L. Solari, B. Sitaud, R. Bes, S. Cammelli, H. Hermange, G. Othmane, S. Safi, P. Moisy, S. Wahu, C. Bresson, M. L. Schlegel, D. Menut, J. L. Bechade, P. Martin, J. L. Hazemann, O. Proux and C. Den Auwer, *Radiochimica Acta*, 2014, **102**, 957-972.
30. B. Ravel and M. Newville, *Journal of Synchrotron Radiation*, 2005, **12**, 537–541.
31. A. L. Ankudinov, B. Ravel, J. J. Rehr and S. D. Conradson, *Physica B: Condensed Matter*, 1998, **58**, 7565−7576.
32. J. M. S. Skakle, C. L. Dickson and F. P. Glasser, *Powder diffraction*, 2000, **15**, 234-238.
33. E. Dalodière, M. Virot, V. Morosini, T. Chave, T. Dumas, C. Hennig, T. Wiss, O. Dieste Blanco, D. K. Shuh, T. Tyliszczak, L. Venault, P. Moisy and S. I. Nikitenko, *Scientific Reports*, 2017, **7**, 43514.
34. A. Paul, *Chemistry of Glasses*, Springer Netherlands, 1982.
35. E. Giffaut, M. Grivé, P. Blanc, P. Vieillard, E. Colàs, H. Gailhanou, S. Gaboreau, N. Marty, B. Madé and L. Duro, *Applied Geochemistry*, 2014 **49**, 225-236.
36. D. Hudry, C. Apostolidis, O. Walter, A. Janßen, D. Manara, J.-C. Griveau, E. Colineau, T. Vitova, T. Prüßmann, D. Wang, C. Kübel and D. Meyer, *Chemistry - A European Journal*, 2014, **20**, 10431-10438.
37. L. Bonato, M. Virot, T. Dumas, A. Mesbah, E. Dalodière, O. Dieste Blanco, T. Wiss, X. Le Goff, M. Odorico, D. Prieur, A. Rossberg, L. Venault, N. Dacheux, P. Moisy and S. I. Nikitenko, *Nanoscale Advances*, 2020, **2**, 214-224.
38. E. Gerber, A. Y. Romanchuk, I. Pidchenko, L. Amidani, A. Rossberg, C. Hennig, G. B. M. Vaughan, A. Trigub, T. Egorova, S. Bauters, T. Plakhova, M. O. J. Y. Hunault, S. Weiss, S. M. Butorin, A. C. Scheinost, S. N. Kalmykov and K. O. Kvashnina, *Nanoscale*, 2020, **12**, 18039-18048.
39. C. Micheau, M. Virot, S. Dourdain, T. Dumas, D. Menut, P. L. Solari, L. Venault, O. Diat, P. Moisy and S. I. Nikitenko, *Environmental Science: Nano*, 2020, **7**, 2252-2266.
40. J. Rothe, C. Walther, M. A. Denecke and T. Fanghänel, *Inorganic Chemistry*, 2004, **43**, 4708-4718.
41. C. L. Ekberg, K., G. Ö.-J. Skarnemark, A. and I. Persson, *Dalton Transactions*, 2013, **42**, 2035-2040
42. R. D. Shannon, *Acta Crystallographica Section A.*, 1976, **32**, 751-767.
43. W. R. Penrose, W. L. Polzer, E. H. Esslngton, D. M. Nelson and K. A. Orlandini, *Environmental Science & Technology*, 1990, **24**, 228-234.
44. R. C. Marty, D. Bennett and P. Thullen, *Environmental Science & Technology*, 1997, **31**, 2020-2027.
45. D. I. Kaplan, P. M. Bertsch, D. C. Adriano and K. A. Orlandini, *Radiochimica Acta*, 1994, **66-67**, 181-187.
46. A. B. Kersting, D. W. Efurd, D. L. Finnegan, D. J. Rokop, D. K. Smith and J. L. Thompson, *Nature*, 1999, **397**, 56-59.
47. A. P. Novikov, S. N. Kalmykov, S. Utsunomiya, R. C. Ewing, F. Horreard, A. Merkulov, S. B. Clark, V. V. Tkachev and B. F. Myasoedov, *Science*, 2006, **314**, 638-641.
48. M. Taylor and R. C. Ewing, *Acta Crystallographica Section B-Structural Crystallography and Crystal Chemistry*, 1978, **34**, 1074-1079.
49. L. H. Fuchs and E. Gebert, *The American Mineralogist*, 1958, **43**, 243-248.